



Long-wavelength fluctuations and anomalous dynamics in 2-dimensional liquids

Yan-Wei Li^a, Chandan K. Mishra^{b,c}, Zhao-Yan Sun^{d,e}, Kun Zhao^f, Thomas G. Mason^{g,h}, Rajesh Ganapathyⁱ, and Massimo Pica Ciamarra^{a,j,1}

^aDivision of Physics and Applied Physics, School of Physical and Mathematical Sciences, Nanyang Technological University, Singapore 637371, Singapore; ^bChemistry and Physics of Materials Unit, Jawaharlal Nehru Centre for Advanced Scientific Research, Jakkur, Bangalore 560064, India; ^cDepartment of Physics and Astronomy, University of Pennsylvania, Philadelphia, PA 19104; ^dState Key Laboratory of Polymer Physics and Chemistry, Changchun Institute of Applied Chemistry, Chinese Academy of Sciences, Changchun 130022, China; ^eUniversity of Science and Technology of China, Hefei 230026, China; ^fKey Laboratory of Systems Bioengineering (Ministry of Education), School of Chemical Engineering and Technology, Tianjin University, Tianjin 300072, China; ^gDepartment of Chemistry and Biochemistry, University of California, Los Angeles, CA 90095; ^hDepartment of Physics and Astronomy, University of California, Los Angeles, CA 90095; ⁱInternational Centre for Materials Science, Jawaharlal Nehru Centre for Advanced Scientific Research, Jakkur, Bangalore 560064, India; and ^jInstitute for Superconductors, Oxides and Other Innovative Materials and Devices, Consiglio Nazionale delle Ricerche, Dipartimento di Scienze Fisiche, Università di Napoli Federico II, I-80126 Napoli, Italy

Edited by Eric R. Weeks, Emory University, Atlanta, GA, and accepted by Editorial Board Member Pablo G. Debenedetti October 1, 2019 (received for review May 30, 2019)

In 2-dimensional systems at finite temperature, long-wavelength Mermin–Wagner fluctuations prevent the existence of translational long-range order. Their dynamical signature, which is the divergence of the vibrational amplitude with the system size, also affects disordered solids, and it washes out the transient solid-like response generally exhibited by liquids cooled below their melting temperatures. Through a combined numerical and experimental investigation, here we show that long-wavelength fluctuations are also relevant at high temperature, where the liquid dynamics do not reveal a transient solid-like response. In this regime, these fluctuations induce an unusual but ubiquitous decoupling between long-time diffusion coefficient D and structural relaxation time τ , where $D \propto \tau^{-\kappa}$, with $\kappa > 1$. Long-wavelength fluctuations have a negligible influence on the relaxation dynamics only at extremely high temperatures in molecular liquids or at extremely low densities in colloidal systems.

long-wavelength fluctuations | diffusion | relaxation | normal liquid

The dimensionality of a system strongly influences the equilibrium properties of its solid phase (1). According to the Mermin and Wagner (2) theorem, indeed, systems with continuous symmetry and short-range interactions lack true long-range translational order at finite temperature, in $d \leq 2$ dimensions. This occurs as in small spatial dimensions the elastic response is dominated by the Goldstone modes, elastic excitations that in the limit of long wavelength (LW) have vanishing energy and a diverging amplitude. A signature of these LW fluctuations is system size-dependent dynamics, which arise as the system size provides a cutoff for the maximum wavelength. This dependence occurs in both ordered and disordered solids, as LW fluctuations are insensitive to the local order (3). This dynamical signature of the LW fluctuations also appears in supercooled liquids, which are liquids cooled below their melting temperature without crystallization occurring. In particular, LW fluctuations affect the transient solid-like response observed in the supercooled regime, which we recap in Fig. 1 via the investigation of the mean-square displacement (MSD), $\langle \Delta r^2(t) \rangle$, and of the self-intermediate scattering function (ISF), $F_s(q, t)$, of the 2-dimensional (2D) modified Kob–Andersen (mKA) system, a prototypical model glass former (*Materials and Methods*). In the supercooled regime the ISF and the MSD develop a plateau revealing a solid-like response in which particles vibrate in cages formed by their neighbors (4). However, this is a transient response, as at longer times the ISF relaxes and the MSD enters a diffusive behavior. Flenner and Szamel (5) have demonstrated that such glassy relaxation dynamics depend on the system size; the signatures of a transient solid-like response disappear in the thermodynamic limit. This trend can be appreciated in Fig. 1, where we com-

pare the dynamics for 3 different system sizes (see also ref. 5 for a full account). Subsequent works have then demonstrated that this size dependence results from the LW fluctuations (3, 6) by showing that the glassy features of the relaxation dynamics are recovered when the effect of LW fluctuations is filtered out (3, 6–8).

A transient solid-like response is observed only below the onset temperature, where the relaxation time exhibits a super-Arrhenius temperature dependence, in fragile systems (*SI Appendix, Fig. S5*), and dynamical heterogeneities (DHs) affect the relation between diffusion coefficient and relaxation time (4). In the normal liquid regime that occurs at higher temperatures in molecular liquids or at lower densities in colloidal systems, the MSD and the ISF do not exhibit plateaus possibly associated with a transient particle localization and are system size independent. This is apparent in Fig. 1, and it suggests that the normal liquid regime is not affected by LW fluctuations. Is this true? And more generally, how far must a system be from the solid phase for its LW fluctuations to have a negligible influence on its relaxation dynamics? Here we show that, surprisingly, LW fluctuations affect the structural relaxation dynamics of 2D systems even in their normal liquid regimes. Specifically, they induce a stretched-exponential relaxation, qualitatively distinct from that observed in the supercooled regime, and an unusual decoupling between the structural relaxation time τ and the long-time diffusion coefficient, D (*Materials and Methods*). This decoupling has been previously observed, both in experiments

Significance

Long-wavelength elastic modes, which have an infinitesimal energy cost, destroy the long-range translational order of 2D solids at finite temperatures. Here we demonstrate that these long-wavelength fluctuations also influence the dynamical properties of 2D systems in their normal liquid regimes. Hence, long-wavelength fluctuations make 2- and 3D molecular particulate systems behave differently from high- to very low-temperature regimes.

Author contributions: K.Z., T.G.M., and M.P.C. designed research; Y.-W.L., C.K.M., Z.-Y.S., and R.G. performed research; and Y.-W.L., K.Z., T.G.M., and M.P.C. wrote the paper.

The authors declare no competing interest.

This article is a PNAS Direct Submission. E.R.W. is a guest editor invited by the Editorial Board.

Published under the PNAS license.

¹To whom correspondence may be addressed. Email: massimo@ntu.edu.sg.

This article contains supporting information online at www.pnas.org/lookup/suppl/doi:10.1073/pnas.1909319116/-DCSupplemental.

First published October 28, 2019.

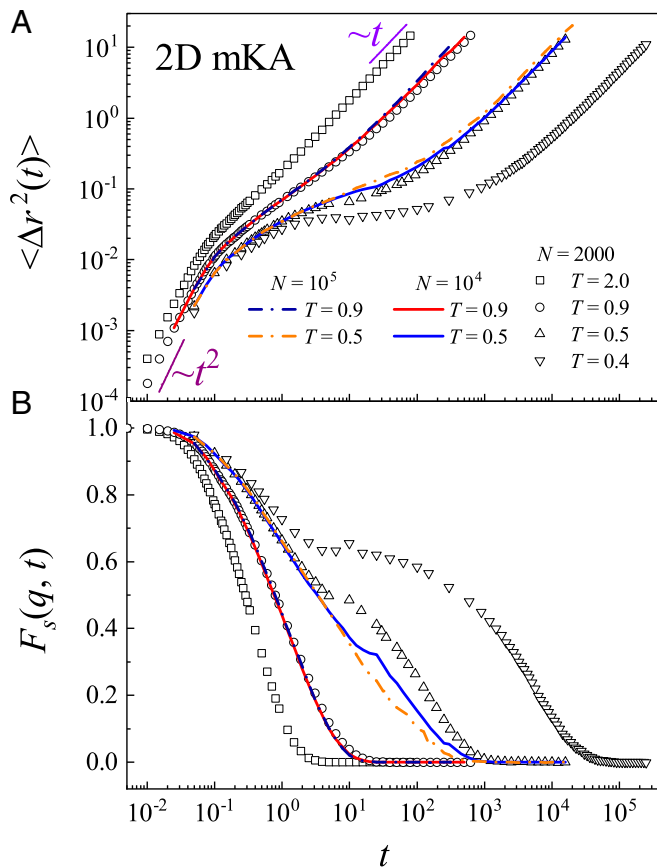


Fig. 1. (A and B) Time dependence of the mean-square displacement (A) and of the self-intermediate scattering function (B) from molecular dynamics simulations of the 2D mKA model. Typical signatures of supercooled dynamics emerge as the temperature T decreases, including ISF oscillations associated with the Boson peak (17). The comparisons of systems with $N = 2,000$, with $N = 10^4$, and with $N = 10^5$ particles (see key defining symbols and lines in A) reveal that the dynamics in the supercooled regime are size dependent (5), while that is not the case in the normal liquid regime.

(9) of colloidal systems and in numerical simulations (10, 11), but its physical origin has remained mysterious. Our results are based on the numerical investigation of the relaxation dynamics of 2 model glass-forming liquids and on the experimental study of a quasi-2D suspension of ellipsoids (9). Numerically, we consider the 3-dimensional (3D) Kob–Andersen (KA) binary mixture (12) and its 2D variant (mKA) (13), as well as the harmonic model (14) (Harmonic) in both 2D and 3D. Numerical details are in *Materials and Methods* and *SI Appendix*. Details on the experimental systems are in refs. 9 and 15. Our results thus demonstrate that LW fluctuations are critical for understanding the properties of 2D systems not only in the crystalline phase (2, 16), the amorphous solid state (3), and the supercooled state (6, 7), but also, surprisingly, in the normal liquid regime.

Results

Dynamics in the 2D Normal Liquid Regime. If the long-time relaxation dynamics of a liquid are not influenced by its energy landscape, as suggested by Fig. 1 and by analogous results for the 2D Harmonic model and 3D KA model reported in *SI Appendix*, Fig. S1, then at the relaxation timescale the displacements of the particles should be uncorrelated and their van-Hove distribution function a Gaussian. This is observed in Fig. 2A, where we plot the dependence of the non-Gaussian parameter α_2 , a common measure of DHs (18) (*Materials and Methods*), on the relaxation

time, for 2D mKA and the 3D KA models. In Fig. 2 and subsequent figures, the shaded area identifies the supercooled regime, as defined in *SI Appendix*, Figs. S5 and S6. Indeed, above the onset temperature $\alpha_2(\tau) \ll 1$ and assumes comparable values in 2D and in 3D. Consistently, the dynamical susceptibility at the relaxation time, $\chi_4(\tau)$, which is a proxy for the presence of correlated spatiotemporal motion (*Materials and Methods*), behaves similarly in 2D and 3D, as in Fig. 2B. However, landscape-independent relaxation dynamics are also expected to lead to an exponential decay of the ISF, $F_s(q, t) \propto \exp[-(t/\tau^e)^\beta]$ with $\beta \simeq 1$. Fig. 2C illustrates that indeed $\beta \simeq 1$ in the normal liquid regime of 3D systems. Conversely, in the 2D normal liquid regime, we observe a stretched exponential relaxation, with $\beta < 1$ decreasing on cooling. The coexistence of a Gaussian van-Hove distribution and a stretched-exponential relaxation is a feature of the antipersistent Gaussian process (19, 20) we show in *SI Appendix*, Fig. S4 to well describe the time evolution of the van-Hove distribution close to the relaxation time. We argue in a following section that this process signals the influence of the LW fluctuations on the relaxation dynamics.

Decoupling between Relaxation and Diffusion. In the supercooled regime, the behavior of the non-Gaussian parameter and the 4-point dynamical susceptibility points toward the coexistence of particles with small and large displacements, on a timescale of the relaxation time. These DHs, a hallmark of the supercooled liquid dynamics (18), induce a breakdown of the inverse relationship between the diffusion coefficient and the structural relaxation time, leading to $D \propto \tau^{-\kappa}$ with $\kappa < 1$, where D and τ are primarily affected by the exhibiting of large and small displacements, respectively. In the normal liquid regime, where the dynamics are not heterogeneous, one therefore might expect $\kappa = 1$ for 2D systems, as commonly observed in 3D systems. Surprisingly, however, in 2D normal liquids one finds $\kappa > 1$ (9–11), for reasons that are currently mysterious. We illustrate the cross-over from the normal liquid regime where $\kappa > 1$ to the supercooled regime where $\kappa < 1$ in Fig. 3 (black squares). Fig. 3 reports results from numerical simulations of the 2D mKA model and of 2D Harmonic discs, as well as results from experiments

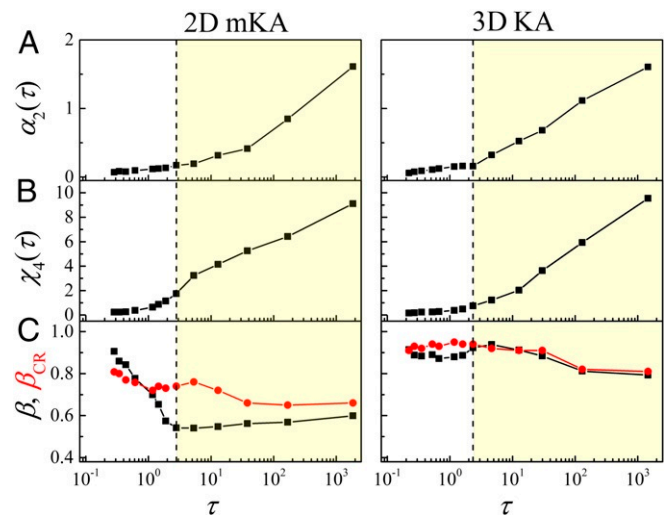


Fig. 2. (A–C) The non-Gaussian parameter $\alpha_2(\tau)$ (A), the 4-point dynamical susceptibility $\chi_4(\tau)$ (B), and the standard β (black squares) and CR β_{CR} (red circles) stretching exponents (C) as functions of relaxation time for the 2D mKA model (Left column) and for the 3D KA system (Right column). The dashed lines mark the relaxation time at the onset temperature. In this and subsequent figures, the yellow shaded region identifies the supercooled regime, as defined in *SI Appendix*, Figs. S5 and S6.

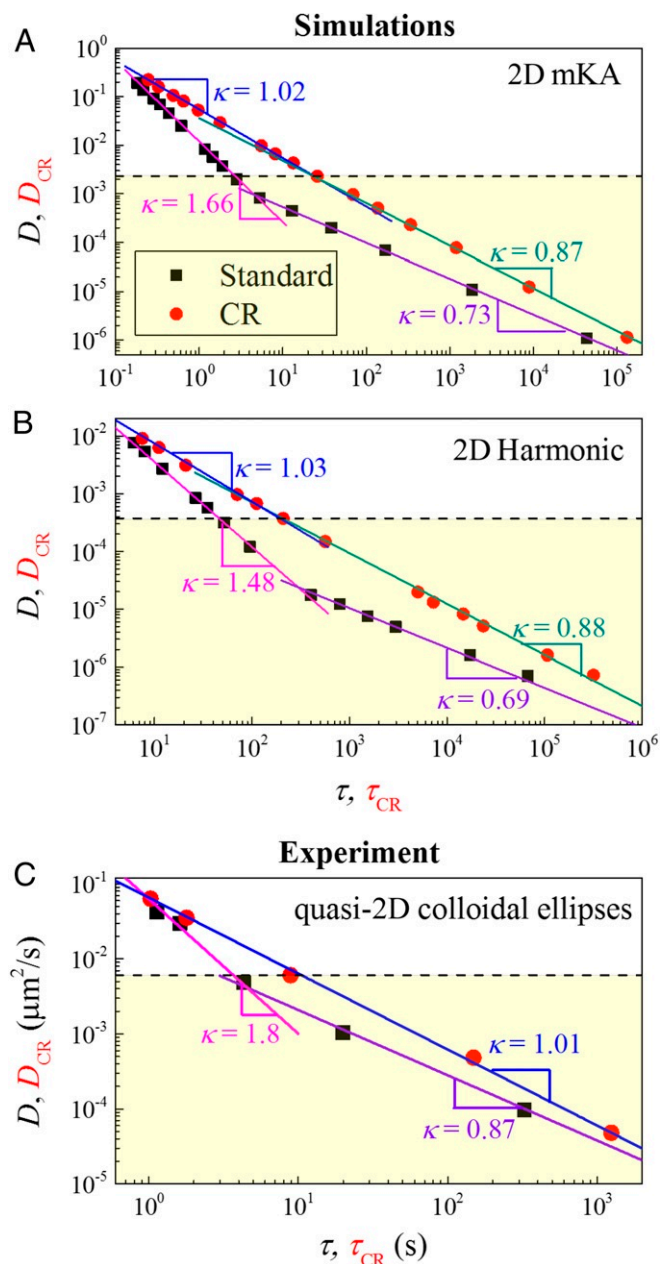


Fig. 3. Dependence of the diffusion coefficient D on the relaxation time τ as obtained by investigating the dynamics using the standard (black squares) and the CR (red circles) measures. **A** refers to the 2D mKA model, **B** to the 2D Harmonic model, and **C** to the experimental quasi-2D colloidal ellipsoids with area fraction $\phi = 0.28, 0.49, 0.68, 0.73,$ and 0.76 . Here and in subsequent figures the horizontal dashed lines mark the size-independent onset point, defined in *SI Appendix*, Figs. S5 and S6.

of quasi-2D colloidal ellipsoids. We find that $\kappa > 1$ occurs in the normal liquid regime, but also extends into the supercooled one (shaded region), as is apparent in Fig. 3B. The reader is warned to take with care the value of κ in the deeply supercooled regime. Indeed, as already shown in Fig. 1, the supercooled regime dynamics are influenced by finite-size effects. Conversely, we stress that results in the normal liquid regime, which is our main focus, are not influenced by finite-size effect, as we show in a subsequent section and in *SI Appendix*.

We provide an insight on the physical origin of the observed $\kappa > 1$ value by investigating the dynamics using cage-relative

(CR) measures (*Materials and Methods*), where the displacement of a particle is evaluated with respect to average displacement of its neighbors. In Fig. 3 we compare the standard and the CR measures by plotting both D vs. τ (black squares) and D_{CR} vs. τ_{CR} (red circles). In the normal liquid regime we find $\kappa > 1$ for the standard measures and $\kappa \simeq 1$ for the CR measures. To better illustrate that there exists an extended range of τ where $\kappa > 1$ for the standard measure and $\kappa = 1$ for the CR measures, we show in *SI Appendix*, Fig. S9 the presence of a plateau region when the product $\tau_{CR} D_{CR}$ is plotted vs. τ_{CR} .

CR measures have been suggested to filter out the effect of the LW fluctuations on the dynamics (6), in the supercooled regime, as they subtract correlated particle displacements. Our results suggest that the LW fluctuations are also responsible for the $\kappa > 1$ behavior. In this respect, note that such a large value of κ indicates that the relaxation time is smaller than expected, given the value of the diffusion coefficient; this effect might possibly arise from the LW fluctuations. Indeed, the LW fluctuations have large amplitudes which, when larger than $\frac{2\pi}{q}$, promote the relaxation of the system but not its diffusion. These oscillations induce an anticorrelated temporal motion, which explains why the high-temperature relaxation dynamics are compatible with those of an antipersistent Gaussian process, a feature of which is the stretched exponential decay of the ISF. Indeed, the CR-ISF, which is not affected by the LW fluctuations, has a higher stretching exponent β which decreases only in the supercooled regime, as in 3D; this is illustrated in Fig. 2C. According to this picture, LW fluctuations affect the relaxation time and not the diffusivity; this interpretation is supported by the results of Fig. 3, from which we understand that the standard and the CR measures mainly differ in their estimates of the relaxation time, which is smaller for the standard measures (see *SI Appendix*, Fig. S1 for a direct comparison of the standard and CR MSD and ISF). The standard and the CR diffusion coefficients have indeed an expected small difference, $D_{CR} = D(1 + 1/N_{nn})$ with N_{nn} the average number of nearest neighbors per particle. We further remark that in the normal liquid regime CR measures have no noticeable size dependence, at variance with what occurs in the deep supercooled regime (21–23).

The above interpretation is also consistent with the investigation of the difference between the standard and the CR measures in 3D. Indeed, Fig. 4 clearly shows that in 3D, where LW fluctuations play a minor role, there are minor differences between the 2 measures, both in the normal liquid and in the supercooled regime.

Long-Wavelength Fluctuations in the 2D Normal Liquid Regime. The above results suggest that in 2D the dynamics of normal liquids are strongly influenced by the LW modes. This is a counterintuitive speculation since the relaxation dynamics are expected to be weakly dependent on the features of the underlying energy

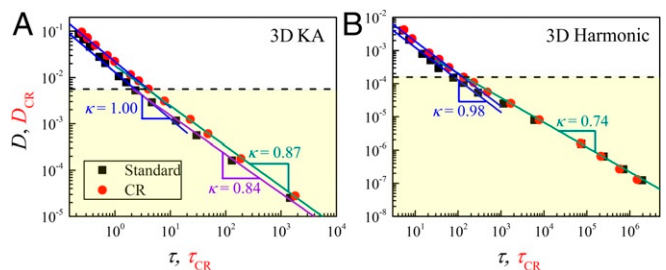


Fig. 4. The same quantities investigated in Fig. 3 are here studied for two 3D systems. **(A)** The 3D KA model. **(B)** The 3D Harmonic model. In 3D $\kappa = 1$ in the normal liquid regime, and there is no difference between the standard and the CR measures.

landscape (4, 24) above the onset temperature. In *SI Appendix, Fig. S10*, we show that the density of states of 2D normal liquids satisfies Debye scaling at LW, thus proving that LW fluctuations exist in this regime. We demonstrate that these LW fluctuations also influence the relaxation dynamics by performing 2 additional investigations.

First, we consider the effect of the microscopic dynamics on the value of κ , comparing the 2 limiting cases of underdamped and overdamped dynamics, corresponding to Langevin dynamics (*SI Appendix*) with Brownian time τ_B respectively much larger and much smaller than the inverse Debye frequency $1/\omega_D$. If the LW modes are responsible for the observed behavior, then the value of κ must depend on the microscopic dynamics, and κ closer to 1 should be obtained for the overdamped dynamics. Indeed, recall that in the solid phase the contribution of modes with frequency ω to the MSD is $r_u^2(t, \omega) = \frac{2k_b T}{m\omega^2} [1 - \cos(\omega t)]$, in the underdamped limit, and $r_o^2(t, \omega) = \frac{2k_b T}{m\omega^2} [1 - e^{-\frac{t}{2\tau_B}}]$ in the overdamped one (25). Accordingly, while in the overdamped limit the contributions of the different modes have the same time dependence, this is not so in the underdamped limit. Specifically, in the underdamped limit, the modes contribute ballistically to the mean-square displacement up to a time $\sim 1/\omega$, which implies that the underdamped dynamics are more strongly affected by the LW modes. Fig. 5 compares the relation between D and τ obtained in the underdamped and in the overdamped limits, for the 2D mKA model, with $\tau_B \omega_D \simeq 100$ and $\simeq 0.01$, respectively, having assumed ω_D to be of the order of the time at which the ballistic regime ends in the Newtonian dynamics (no damping). The underdamped results are analogous to those of the previously considered Newtonian dynamics reported in Fig. 34, as expected. Conversely, the overdamped results strongly differ in that $\kappa \simeq 1$ is essentially recovered in the normal liquid regime. This agrees with our theoretical argument and clarifies that the decoupling behavior with $\kappa > 1$ is the combined effect of the presence of LW modes and of the specific microscopic dynamics through which the system explores its phase space.

As a second check we explicitly evaluate the relevance of the LW modes to the overall particle displacement, as a function of time. To this end, we project the normalized displacement $\widehat{\Delta \mathbf{r}}(t) = \Delta \mathbf{r}(t)/|\Delta \mathbf{r}(t)|$ of the particles at time t on the eigenvectors $u_i(\omega_i)$ of the Hessian matrix of the nearest inherent configuration (*Materials and Methods*) of the $t=0$ configuration: $\widehat{\Delta \mathbf{r}}(t) = \sum_i \beta_i(t) \mathbf{u}_i(\omega_i)$. $\beta_i^2(t)$ is therefore the relative contribution of mode i to the overall displacement at time t . To assess the relevance of the LW modes we compute the contribution of the 0.75% modes with the longest wavelength, $W_{0.75\%}(t) = \sum_i \beta_i^2(t)$. Fig. 6 compares $W_{0.75\%}(t)$ for the underdamped and the overdamped dynamics, both in the liquid and in the supercooled regime. In both regimes, 0.75% of the longest-wavelength

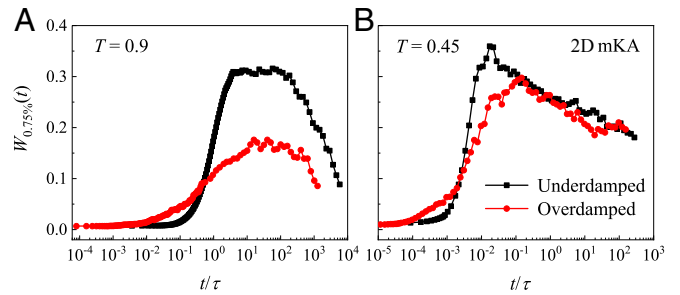


Fig. 6. Contribution of the 0.75% of the modes with the longest wavelength to the particle displacement, as a function of time, for a system evolving with the underdamped (black squares) and overdamped (red circles) dynamics. (A) $T = 0.9$, in the normal liquid regime. (B) $T = 0.45$, in the supercooled regime. The data are for the 2D mKA system and are obtained by averaging over 30 independent runs.

modes contribute more than 30% of the overall displacement. This is a clear indication that LW fluctuations are extremely relevant, also in the normal liquid regime. Consistent with our previous finding, we also find the contribution of the LW modes to be more relevant for the underdamped than for the overdamped dynamics. Besides, in the underdamped regime, for low frequencies $\beta_i(t)$ has a transient oscillatory behavior in line with the presence of transient solid-like modes, also in the liquid regime.

Viscosity and Size Effects. The study of the shear viscosity η , which is the Green-Kubo integral (26) of the shear stress autocorrelation function (*SI Appendix, Fig. S3*), offers an alternative approach to filter out the effect of the LW fluctuations. This is because the stress is insensitive to the LW fluctuations, as it depends on the interparticle forces and hence on the relative distances between the particles. Indeed, Fig. 7 shows

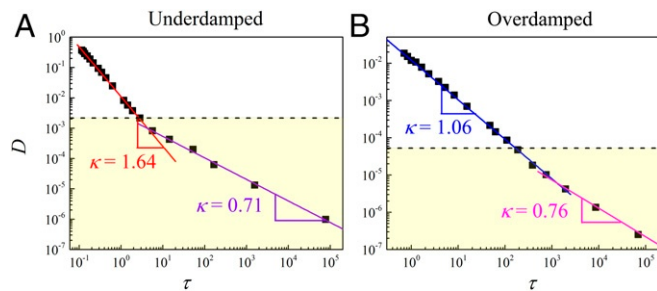


Fig. 5. Dependence of the diffusion coefficient D on the relaxation time τ for the 2D mKA model. In A, the system evolves according to underdamped dynamics, and $\kappa > 1$ is observed in the normal liquid regime, while in B it evolves according to overdamped dynamics, and $\kappa \simeq 1$.

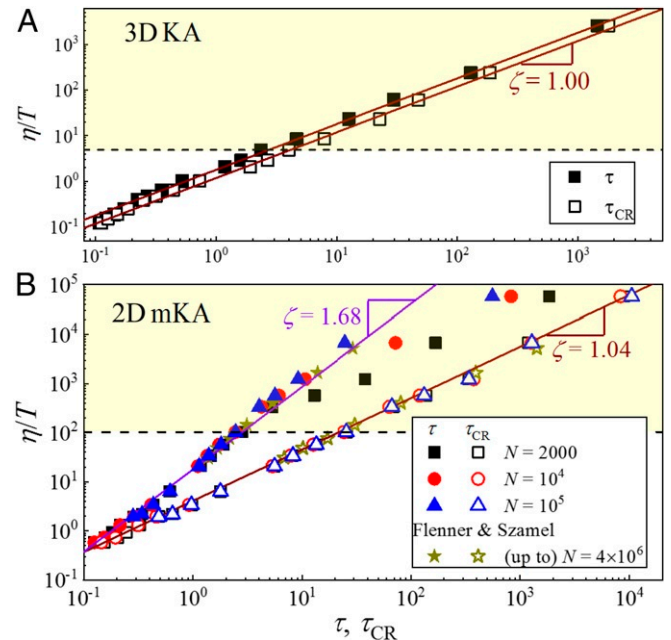


Fig. 7. Dependence of the ratio η/T on the relaxation time τ (solid symbols) and on the CR relaxation time τ_{CR} (open symbols). A shows data for the 3D KA model. B illustrates data for the 2D mKA model and compares different system sizes using our own data and data from ref. 21. The horizontal dashed lines in both A and B mark η/T at the onset temperature.

that η/T is proportional to τ_{CR} for both the 3D KA and the 2D mKA models (open symbols). In 3D, $\tau_{CR} \sim \tau$, and hence $\eta/T \propto \tau$ (Fig. 7, solid symbols), as also previously reported (10, 27). Differently, in the 2D normal liquid regime $\eta/T \propto \tau^\zeta$ with $\zeta \simeq \kappa$ (Fig. 3A). This result indicates that 2D and 3D systems behave analogously concerning the breakdown of the Stokes–Einstein (SE) relation $D \propto T/\eta$. This relation holds in the normal liquid, where $D \propto \tau^{-\kappa}$ and $\eta/T \propto \tau^\zeta$, with $\kappa \simeq \zeta = 1$ in 3D and $\kappa \simeq \zeta > 1$ in 2D. Conversely, the SE relation breaks down in the supercooled regime where $\kappa < 1$, as $\zeta \simeq 1$ in 3D and $\zeta > 1$ in 2D.

Fig. 7B demonstrates that size effects diminish as the system size increases, as we highlight also considering data from ref. 21 for systems with up to 4 million particles, and become negligible for large enough systems. This behavior results from the competition of 2 timescales. One timescale is the CR relaxation time $\tau_{CR}(T)$, which is essentially size independent. The other timescale is the typical timescale of the LW modes. Since the longest wavelength is proportional to the system size, this timescale varies as $\tau_{LW}(L) \propto L$, as we verify in *SI Appendix, Fig. S11*. Finite system size effects, which are present when the LW modes develop before the system relaxes, $\tau_{CR}(T) \gg \tau_{LW}(L)$, thus vanish as the system size increases. Fig. 7B also clarifies that for the 2D mKA model, above the onset temperature size effects are lost in our smallest system. Therefore, all our results obtained in the liquid regime do not suffer from finite system size effects.

Discussion

In conclusion, our results indicate that LW fluctuations affect the structural relaxation of 2D liquids in the normal liquid regime, where the relaxation dynamics do not suggest a transient solid response, even when evaluated using CR measures (*SI Appendix, Fig. S1*). In this regime, the LW fluctuations induce stretched exponential relaxations qualitatively different from those observed in the supercooled regime, which is not associated with the coexistence of particles with markedly different displacements. This result allows us to rationalize an open issue in the literature (9–11), namely the physical origin of the decoupling between relaxation and diffusion $D \propto \tau^{-\kappa}$ with $\kappa > 1$. In the main text, we have presented numerical data for the 2D mKA model and the 2D Harmonic model and their 3D counterpart for comparison, as well as experimental data for a 2D suspension of hard ellipses. We note, however, that we have also observed consistent results in a binary system with inverse power-law potential (28) and in monodisperse systems of Penrose kites (29, 30) (*SI Appendix, Fig. S15*). Thus, our findings appear extremely robust as they do not depend on whether the interaction potential is finite or diverging at the origin, attractive or purely repulsive, or isotropic or anisotropic.

It is natural to ask whether, at high enough temperature or low enough density, the effect of LW fluctuations becomes negligible. The answer to this question is affirmative. Indeed, we do see in Fig. 3 that the difference between the standard and the CR measures, which is a proxy for the relevance of LW fluctuations, decreases as the relaxation time decreases. In the numerical model we have explicitly verified that the 2 measures coincide in this very high-temperature limit (*SI Appendix, Fig. S1*). Interestingly, in the Harmonic model, where the potential is bounded, we have found that in this limit the system relaxes before the ballistic regime of the MSD ends. This leads to $D \propto \tau^{-\kappa}$ and $\kappa = 2$, in both 2D and 3D, as we discuss and verify in *SI Appendix, Fig. S2*. We checked in *SI Appendix, Figs. S7 and S8* that the value $\kappa > 1$ we have attributed to the LW fluctuations is not conversely the signature of a cross-over from the normal to the high-temperature liquid. In colloidal sys-

tems, particles perform independent Brownian motions in the low-density limit, where LW fluctuations are therefore negligible. We expect the cross-over density below which LW fluctuations are negligible to depend on the viscoelasticity of the solvent.

We conclude with 2 more remarks. First, it is established that CR measures remove the effect of LW fluctuations (3, 6). Here we note that CR measures filter out all correlated displacements between close particles, regardless of their physical origin. In particular, in the supercooled regime, they suppress the effect of correlated particle displacements arising from DHs (see *SI Appendix, Fig. S12* for the comparison of the 4-point dynamical susceptibility between standard and CR measures). This has to be taken into account when using 2D systems to investigate the glass transition. We note that it appears difficult to selectively suppress only the correlations arising from 1 of these 2 physical processes, as DHs are associated with the low-frequency vibrational modes (31). In this respect, perhaps one may consider that DHs in the supercooled regime are associated with localized modes, while LW fluctuations are signatures of extended modes.

Finally, we highlight that LW fluctuations are found in quasi-2D colloidal experiments of both spherical (3, 6) and ellipsoidal (32) particles, as we have shown. However, we have found no clear evidence of LW fluctuations in our overdamped numerical simulations. Hence, the overdamped simulations do not fully describe the behavior of colloidal suspensions. This is not a surprise, as it is indeed well known (33–37) that, due to the presence of hydrodynamic interactions, the velocity autocorrelation function of colloidal systems does not decay exponentially as in the numerical simulations of the overdamped dynamics. The upshot of this consideration is that collective vibrations observed in colloidal systems, including the LW fluctuations, may stem from the hydrodynamic interparticle interaction. It would be of interest to better characterize these collective hydrodynamic induced modes.

Materials and Methods

Model Systems. In 2D, we investigated the mKA model (13) and the harmonic model (14). The mKA model is a 65(A):35(B) mixture, with interaction potential $U_{\alpha\beta}(r) = 4\epsilon_{\alpha\beta}[(\sigma_{\alpha\beta}/r)^{12} - (\sigma_{\alpha\beta}/r)^6 + C_{\alpha\beta}]$, when $r \leq r_{\alpha\beta} = 2.5\sigma_{\alpha\beta}$, and $U_{\alpha\beta}(r) = 0$ otherwise. Here, $\alpha, \beta \in \{A, B\}$. The interaction parameters are given by $\sigma_{AB}/\sigma_{AA} = 0.8$, $\sigma_{BB}/\sigma_{AA} = 0.88$, $\epsilon_{AB}/\epsilon_{AA} = 1.5$, and $\epsilon_{BB}/\epsilon_{AA} = 0.5$. $C_{\alpha\beta}$ guarantees $U_{\alpha\beta}(r_{\alpha\beta}) = 0$. The number density is $\rho = 1.2$. Length, energy, and time are recorded in units of σ_{AA} , ϵ_{AA} , and $\sqrt{m\sigma_{AA}^2/\epsilon_{AA}}$, respectively. For this model, we consider $N = 2,000$ (if not otherwise stated), $N = 10^4$, and $N = 10^5$. The Harmonic model (14) is a 50:50 mixture of $N = 3,000$ particles with interaction potential $U_{\alpha\beta}(r) = 0.5\epsilon(1 - r/\sigma_{\alpha\beta})^2$, for $r < \sigma_{\alpha\beta}$, and $U_{\alpha\beta}(r) = 0$ otherwise. The size ratios are $\sigma_{AB}/\sigma_{AA} = 1.2$ and $\sigma_{BB}/\sigma_{AA} = 1.4$, and the number density is $\rho = 0.699$. The units for energy, length, and time are ϵ , σ_{AA} , and $\sqrt{m\sigma_{AA}^2/\epsilon}$, respectively. In 3D, we simulated the KA model (12), which consists of $N = 3,074$ with 80% A and 20% B particles, as well as the Harmonic model, with $N = 3,000$. All of the results are averaged over at least 4 independent runs. We show the data for A particles if the system is a binary mixture.

We have performed Newtonian dynamics in different thermodynamic ensembles, as well as using a Langevin dynamics, as detailed in *SI Appendix*. All simulations are performed with the GPU-accelerated GALAMOST package (38).

Calculation Details. The MSD is $\langle \Delta r^2(t) \rangle = \langle \frac{1}{N} \sum_{i=1}^N \Delta r_i(t)^2 \rangle$, where $\Delta r_i(t) = r_i(t) - r_i(0)$ is the displacement of particle i at time t . Its long-time behavior defines the diffusion coefficient $D = \lim_{t \rightarrow \infty} \frac{\langle \Delta r^2(t) \rangle}{2dt}$, with d the dimensionality. The ISF is $F_s(q, t) = \langle \frac{1}{N} \sum_{i=1}^N e^{iq \cdot \Delta r_i(t)} \rangle$ with $q = |q|$ the wavenumber of the first peak of the static structure factor. The relaxation time τ is such that $F_s(q, \tau) = e^{-1}$. We have verified in *SI Appendix, Figs. S13 and S14* that our results are robust with respect to the definition of τ . The non-Gaussian parameter is $\alpha_2(t) = \frac{\langle \Delta x(t)^4 \rangle}{3\langle \Delta x(t)^2 \rangle^2} - 1$ with $\Delta x(t)$ the

displacement in the x coordinate (18). Finally, the 4-point dynamical susceptibility $\chi_4(t)$ is defined as $\chi_4(t) = N[\langle \tilde{F}_s(q, t)^2 \rangle] - \langle \tilde{F}_s(q, t) \rangle^2$, with $\tilde{F}_s(q, t) = 1/N \sum_{j=1}^N e^{iq \cdot \Delta r_j(t)}$.

CR quantities are defined by replacing the standard displacement $\Delta r_i(t)$ with the CR one, $\Delta r_i^{CR}(t) = r_i(t) - r_i(0) - 1/N_i \sum_{j=1}^{N_i} [r_j(t) - r_j(0)]$ with N_i the number of neighbors of particle i evaluated at time 0. Neighbors are identified via a Voronoi construction.

Results of Fig. 6 are obtained by projecting the normalized particle displacement at time t on the modes of the inherent structures of the $t=0$ configurations. We have obtained these modes by minimizing the energy

- P. M. Chaikin, T. C. Lubensky, *Principles of Condensed Matter Physics* (Cambridge University Press, 1995).
- N. D. Mermin, H. Wagner, Absence of ferromagnetism or antiferromagnetism in one- or two-dimensional isotropic Heisenberg models. *Phys. Rev. Lett.* **17**, 1133–1136 (1966).
- B. Illing *et al.*, Mermin–Wagner fluctuations in 2D amorphous solids. *Proc. Natl. Acad. Sci. U.S.A.* **114**, 1856–1861 (2017).
- P. G. Debenedetti, F. H. Stillinger, Supercooled liquids and the glass transition. *Nature* **410**, 259–267 (2001).
- E. Flenner, G. Szamel, Fundamental differences between glassy dynamics in two and three dimensions. *Nat. Commun.* **6**, 7392 (2015).
- S. Vivek, C. P. Kelleher, P. M. Chaikin, E. R. Weeks, Long-wavelength fluctuations and the glass transition in two dimensions and three dimensions. *Proc. Natl. Acad. Sci. U.S.A.* **114**, 1850–1855 (2017).
- H. Shiba, Y. Yamada, T. Kawasaki, K. Kim, Unveiling dimensionality dependence of glassy dynamics: 2d infinite fluctuation eclipses inherent structural relaxation. *Phys. Rev. Lett.* **117**, 245701 (2016).
- H. Shiba, P. Keim, T. Kawasaki, Isolating long-wavelength fluctuation from structural relaxation in two-dimensional glass: Cage-relative displacement. *J. Phys. Condens. Matter* **30**, 094004 (2018).
- C. K. Mishra, R. Ganapathy, Shape of dynamical heterogeneities and fractional Stokes-Einstein and Stokes-Einstein-Debye relations in quasi-two-dimensional suspensions of colloidal ellipsoids. *Phys. Rev. Lett.* **114**, 198302 (2015).
- S. Sengupta, S. Karmakar, C. Dasgupta, S. Sastry, Breakdown of the Stokes-Einstein relation in two, three, and four dimensions. *J. Chem. Phys.* **138**, 12A548 (2013).
- J. Kim, B. J. Sung, Tracer shape and local media structure determine the trend of translation-rotation decoupling in two-dimensional colloids. *Phys. Rev. Lett.* **115**, 158302 (2015).
- W. Kob, H. C. Andersen, Scaling behavior in the β -relaxation regime of a supercooled Lennard-Jones mixture. *Phys. Rev. Lett.* **73**, 1376–1379 (1994).
- R. Brüning, D. A. St-Onge, S. Patterson, W. Kob, Glass transitions in one-, two-, three-, and four-dimensional binary Lennard-Jones systems. *J. Phys. Condens. Matter* **21**, 035117 (2009).
- C. S. O'Hern, L. E. Silbert, A. J. Liu, S. R. Nagel, Jamming at zero temperature and zero applied stress: The epitome of disorder. *Phys. Rev. E* **68**, 011306 (2003).
- C. K. Mishra, A. Rangarajan, R. Ganapathy, Two-step glass transition induced by attractive interactions in quasi-two-dimensional suspensions of ellipsoidal particles. *Phys. Rev. Lett.* **110**, 188301 (2013).
- K. J. Strandburg, Two-dimensional melting. *Rev. Mod. Phys.* **60**, 161–207 (1988).
- K. Binder, W. Kob, *Glassy Materials and Disordered Solids* (World Scientific, 2011), Revised edition.
- E. R. Weeks *et al.*, Three-dimensional direct imaging of structural relaxation near the colloidal glass transition. *Science* **287**, 627–631 (2000).
- J. P. Bouchaud, "Anomalous relaxation in complex systems: From stretched to compressed exponentials" in *Anomalous Transport: Foundations and Applications*, R. Klages, G. Radons, I. M. Sokolov, Eds. (John Wiley & Sons, Ltd, 2008), pp. 327–345.
- B. B. Mandelbrot, J. W. V. Ness, Fractional Brownian motions, fractional noises and applications. *SIAM Rev.* **10**, 422–437 (1968).
- E. Flenner, G. Szamel, Viscoelastic shear stress relaxation in two-dimensional glass-forming liquids. *Proc. Natl. Acad. Sci. U.S.A.* **116**, 2015–2020 (2019).
- B. J. Alder, T. E. Wainwright, Decay of the velocity autocorrelation function. *Phys. Rev. A* **1**, 18–21 (1970).
- H. Shiba, T. Kawasaki, K. Kim, Local density fluctuation governs divergence of viscosity underlying elastic and hydrodynamic anomalies in 2d glass-forming liquid. arXiv:1905.05458 (14 May 2019).
- S. Sastry, P. G. Debenedetti, F. H. Stillinger, Signatures of distinct dynamical regimes in the energy landscape of a glass-forming liquid. *Nature* **393**, 554–557 (1998).
- M. C. Wang, G. E. Uhlenbeck, On the theory of the Brownian motion. *Rev. Mod. Phys.* **17**, 323–342 (1945).
- J. P. Hansen, I. R. McDonald, *Theory of Simple Liquids* (Academic Press, London, UK, ed. 3, 2005).
- T. Kawasaki, K. Kim, Identifying time scales for violation/preservation of Stokes-Einstein relation in supercooled water. *Sci. Adv.* **3**, e1700399 (2017).
- D. N. Perera, P. Harrowell, Origin of the difference in the temperature dependences of diffusion and structural relaxation in a supercooled liquid. *Phys. Rev. Lett.* **81**, 120–123 (1998).
- K. Zhao, T. G. Mason, Shape-designed frustration by local polymorphism in a near-equilibrium colloidal glass. *Proc. Natl. Acad. Sci. U.S.A.* **112**, 12063–12068 (2015).
- Y. Zong, K. Chen, T. G. Mason, K. Zhao, Vibrational modes and dynamic heterogeneity in a near-equilibrium 2D glass of colloidal kites. *Phys. Rev. Lett.* **121**, 228003 (2018).
- A. Widmer-Cooper, H. Perry, P. Harrowell, D. R. Reichman, Irreversible reorganization in a supercooled liquid originates from localized soft modes. *Nat. Phys.* **4**, 711–715 (2008).
- B. Zhang, X. Cheng, Long-wavelength fluctuations and static correlations in quasi-2D colloidal suspensions. *Soft Matter* **15**, 4087–4097 (2019).
- D. A. Weitz, D. J. Pine, P. N. Pusey, R. J. A. Tough, Nondiffusive Brownian motion studied by diffusing-wave spectroscopy. *Phys. Rev. Lett.* **63**, 1747–1750 (1989).
- J. X. Zhu, D. J. Durian, J. Müller, D. A. Weitz, D. J. Pine, Scaling of transient hydrodynamic interactions in concentrated suspensions. *Phys. Rev. Lett.* **68**, 2559–2562 (1992).
- T. G. Mason, D. A. Weitz, Optical measurements of frequency-dependent linear viscoelastic moduli of complex fluids. *Phys. Rev. Lett.* **74**, 1250 (1995).
- J. K. G. Dhont, *An Introduction to Dynamics of Colloids* (Elsevier, 1996).
- T. Li, M. G. Raizen, Brownian motion at short time scales. *Ann. Phys.* **525**, 281–295 (2013).
- Y. L. Zhu *et al.*, GALAMOST: GPU-accelerated large-scale molecular simulation toolkit. *J. Comput. Chem.* **34**, 2197–2211 (2013).